

Augmented-space recursive method for the study of short-ranged ordering effects in binary alloys

Tanusri Saha, Indra Dasgupta, and Abhijit Mookerjee

S.N. Bose National Centre for Basic Sciences, DB-17, Sector 1, Salt Lake City, Calcutta 700064, India

(Received 23 March 1994; revised manuscript received 13 July 1994)

We propose a combination of the generalized augmented-space theorem and the recursion method of Haydock *et al.* to study short-ranged ordering effects in binary alloys. We apply this technique to a tight-binding linear muffin-tin orbitals study of 50-50 AgPd and 50-50 paramagnetic FeNi and predict ordering in the former and segregation in the latter. This is in qualitative agreement with earlier embedded-cluster methods.

I. INTRODUCTION

Ordering or segregation phenomena in binary alloys and their electronic properties are closely related to each other. The electronic energy is order dependent and, in turn, causes the formation and stability of ordered, disordered, and segregated structures. We shall address the important problem of developing a first-principles theory for predicting the tendency of ordering or segregation from electronic structure calculations. The tendency of ordering or segregation is governed by correlations in concentration between the neighboring sites expressed in terms of the Warren-Cowley short-range order parameter. Such correlation between constituent species is directly related to the behavior of diffuse scattering and can be obtained from the quantitative intensity measurements on a single crystal. One needs a self-consistent first-principles theory of correlated disorder in order to analyze such ordering tendencies.

The most successful theoretical tool to date for understanding the electronic structure of disordered alloys is the coherent potential approximation (CPA).¹ Because of the single-site character of its averaging procedure, the CPA cannot account for local ordering effects. An adequate theory requires a more complex averaging scheme which will take into account the effect of clusters and at the same time retain the proper analytic form of the Green function. Several attempts at extension of the CPA in order to take cluster effects into account have been reported to date.

Among such past attempts are the molecular CPA (MCPA) (Ref. 2) and theories like the surrounded atom model.³ In the MCPA, the effective potential is defined by the condition that a single cell, as opposed to a single site, is embedded in the effective medium, in such a way that it produces no further scattering on the average. However, applications of the MCPA to binary metallic alloys are limited by the absence of an appropriate molecular unit. In the surrounded atom model, severe simplification was made by simulating the environment of a real cluster by a Bethe lattice of same coordination number. In recent times, a major development in this direction is the embedded cluster method⁴ in which one solves for the Green function of a cluster of real atoms embedded in an effective medium which is determined

within the single-site CPA. The electronic structure is determined for all possible inequivalent configurations of the cluster and finally the average electronic density of states for a given value of the short-ranged order parameter is determined by direct averaging with an appropriate statistical weight consistent with the short-range order parameter. The theory is not self-consistent. Although in this theory one retains scattering effects from the cluster, the medium in which it is embedded contains no correlated scattering.

It is clear from the preceding discussion that in order to treat systems with correlated disorder, one needs to go beyond the single-site CPA. The augmented-space formalism (ASF) for configuration averaging put forward by one of us⁵ provides a systematic method for the cluster generalizations of the CPA resulting in a Herglotz⁶ Green function. In the augmented-space formalism, one constructs a nonrandom Hamiltonian defined on a new Hilbert space (the augmented space) which is a direct product of the Hilbert space spanned by the original Hamiltonian basis set and the configuration space which is spanned by the various allowed configuration states of the disordered Hamiltonian. The theorem then relates the average of any function of the Hamiltonian to a matrix element on a particular subspace of the augmented space. This configuration averaging in the augmented space is *exact* and does not involve any single-site approximation as in the CPA and treats both diagonal and off-diagonal disorders on equal footing. Controlled approximations on the Green functions are introduced *after* the averaging and can be designed to preserve the necessary Herglotz properties. Recently, the ASF has been employed to derive cluster generalizations of the CPA (CCPA) in the framework of first-principles methods like the Korringa-Kohn-Rostocker⁷ (KKR) and tight-binding linear-muffin-tin orbital⁸ (TB-LMTO), but to date all applications have been confined to specific model systems.

The application of the ASF to correlated disorder was first attempted by Gray and Kaplan.⁹ These authors employed measure theoretical arguments to express the joint probability distribution of the dependent random variables in terms of the product of the probability distributions of individual variables and an auxiliary function to take into account the correlations in probability (this is the Radon-Nikodym derivative). The resulting

configuration-averaged Green function was obtained by the use of the augmented-space theorem and was expressed as an infinite series expansion in terms of Green functions with uncorrelated random variables. Although the full series expansion was proved by Gray and Kaplan to yield a *Herglotz* Green function, once the series is truncated (as one must do, in any practical calculation) there is no guarantee that *herglozicity* will be preserved. The same methodology was used by Razee and Prasad¹⁰ within a KKR-CCPA framework and applied to a simple model of s states on a linear chain. Indeed they found that because of the truncation procedure, negative density of states resulted in certain ranges of the short-ranged order parameter.

A generalized augmented-space formalism (GASF) has recently been proposed by Mookerjee and Prasad¹¹ to deal with correlated disorder. In the present work we apply this formalism coupled with the recursion technique of Haydock *et al.*¹² The formalism bears a close resemblance that of Gray and Kaplan. However, the effect of short-ranged ordering is incorporated within the construction of the operators $M^{(i)}$ themselves. The Radon-Nikodym transformation is not used and there is no expansion necessary in an infinite series. Consequently no truncation is required. The recursive technique proposed by us contrasts with the partitioning technique used by Datta *et al.*⁸ The number of coupled self-consistent equations involved in the partitioning technique rapidly increases as the size of the cluster used in the partitioning is increased. This makes practical implementation not feasible. The direct recursion on augmented space does not possess this restriction.

In spite of its immense potentiality, the ASF recursion could not be implemented in a real alloy system successfully earlier because of the large rank of the augmented Hamiltonian. For a binary alloy with N sites and with only s orbitals it is $(N \times 2^N) \times (N \times 2^N)$. Recently¹³ this formalism has been implemented for describing the electronic structure of random alloys with uncorrelated disorder. The local point-group symmetries of the underlying lattice and larger symmetries in the full augmented space arising out of homogeneity of the disorder have been exploited to make the method tractable. This has been discussed in detail in our earlier work.¹³

Unlike the embedded-cluster method where the configuration averaging for each realization of the embedded cluster is done by explicit averaging over all the distinct configurations (144 for a fcc lattice with first shell of neighbors), this generalized augmented-space recursion technique yields, in a single recursion, the configuration average directly. We apply this methodology to study two distinct alloy systems AgPd and FeNi.

The rest of the paper is organized as follows. In Sec. II, we briefly describe the generalized augmented-space formalism for correlated variables in a form that lends itself directly to its application in recursion technique presented in Sec. III. Section IV is concerned with computational details. Section V is devoted to results and discussion where we apply our methodology to AgPd and paramagnetic FeNi alloys to test the tendency of ordering or segregation in these alloys.

II. THE GENERALIZED AUGMENTED-SPACE FORMALISM

The generalized augmented-space formalism for correlated disorder has been derived and discussed extensively by Mookerjee and Prasad.¹¹ In this section we present those salient features of their methodology which will be of direct use in our application. We shall first present the method for the independent random variables and then we will discuss its generalization to the correlated random variables.

As mentioned in the Introduction, the augmented-space formalism for the configuration averaging is done by extending the usual Hilbert space H to include a configuration space Φ . Disorder effects are described in Φ .

Let $\{n_i\}$ be a collection of discrete independent random variables and $f(n_1, n_2, n_3, \dots)$ be some function of these random variables. Each random variable n_i takes on values $m_1, m_2, \dots, m_\alpha$ and one can decompose the joint probability distribution function of the variables $\{n_i\}$. $P(\{n_i\})$ as

$$P(n_1 \cdots n_r \cdots) = p_1(n_1) \cdots p_r(n_r) \cdots$$

Each $p_i(n_i)$ is positive definite and has finite moments to all orders. For each density $p_i(n_i)$, a Hilbert space ϕ_i , spanned by the states of n_i , is constructed and the full system configuration space is defined as $\Phi = \prod \phi_i$. To each random variable n_i a self-adjoint operator $M_i \in \phi_i$ is associated, such that

$$p_i(n_i) = -1/\pi \text{Im} \langle v_0^i | (n_i I - M_i)^{-1} | v_0^i \rangle, \quad (1)$$

where $|v_0^i\rangle = \sqrt{(1/\alpha)} \sum_{j=1}^{\alpha} |m_j^i\rangle$ is a specific member of ϕ_i . We define the *ground state* $|v_0\rangle$ in product space Φ as $|v_0\rangle = |v_0^1\rangle \otimes |v_0^2\rangle \otimes \cdots$.

The augmented-space theorem states that the configuration average

$$\langle f \rangle_{\text{av}} = \langle v_0 | f(\tilde{M}^{(1)}, \tilde{M}^{(2)}, \dots, \tilde{M}^{(i)} \cdots) | v_0 \rangle,$$

where

$$\tilde{M}^{(i)} = I \otimes \cdots \otimes M_i \cdots \otimes I \otimes \cdots \quad (2)$$

and \tilde{f} is the same function of $\tilde{M}^{(i)}$'s as f was of n_i 's. This expresses the expectation value of \tilde{f} in terms of fixed non-random quantities. The calculation of $\langle f \rangle_{\text{av}}$ thus reduces to the problem of obtaining this expectation value.

If the variables $\{n_i\}$ instead of being independent are correlated then the joint probability distribution of all the variables

$$P(n_1, n_2, n_3, \dots) = p_1(n_1) p_2(n_2 | n_1) p_3(n_3 | n_2, n_1) \cdots \quad (3)$$

In general for the variable n_r , one has an associated \tilde{M}_r of the form,

$$\tilde{M}^{(i)} = \sum_{k_1} \cdots \sum_{k_{i-1}} P_1^{k_1} \otimes P_2^{k_2} \otimes \cdots \otimes M_i^{k_1, \dots, k_{i-1}} \otimes I \otimes \cdots, \quad (4)$$

where, the operator $M_i^{k_1, \dots, k_{i-1}}$ is associated with the conditional probability density $p_i(n_i | n_1 = m_{k_1}^1, \dots, n_{i-1} = m_{k_{i-1}}^{i-1})$ and $P_i^{k_i}$ are projection operators on a specific state k_i . The basic augmented-space theorem still holds good rigorously, but $\tilde{M}^{(i)}$ instead being of the form given by (2), now has the form given by (4). For electronic structure calculations in a disordered system, f is chosen to be the matrix element of the Green function $(zI - H)^{-1}$, where H describes the random Hamiltonian of the system and n_i are the site occupation variables.

We shall now make the assumption that the short-range order effect is restricted to first-nearest-neighbor shell *alone*. This is a reasonable choice based on the fact that short-range order decreases rapidly with distance. Hence, the variables associated with sites beyond first-nearest-neighbor shell will be assumed to be random with no correlation with the central site.

The macroscopic state of order for a binary alloy is described in terms of the Warren-Cowley short-range-order parameter

$$\alpha_r^{AB} = 1 - \frac{P_r^{AB}}{y}, \quad (5)$$

where the A atom is at the center of the r th shell, y denotes the macroscopic concentration of species B , and P_r^{AB} is the pair probability of finding a B atom anywhere in the r th shell around an A atom.

The probability density associated with the sites belonging to the first-nearest-neighbor shell is given by

$$\begin{aligned} p(n_{R_2} | n_{R_1} = 0) &= (y + \alpha x) \delta(n_{R_2}) + (1 - \alpha)x \delta(n_{R_2} - 1), \\ p(n_{R_2} | n_{R_1} = 1) &= (x + \alpha y) \delta(n_{R_2} - 1) + (1 - \alpha)y \delta(n_{R_2}), \end{aligned} \quad (6)$$

where n_R is the variable associated with central atom and $\alpha = \alpha_1^{AB}$.

The construction of different operators in augmented-space associated with the site occupation variables has been discussed in detail by Mookerjee and Prasad. We mention here only the form of augmented-space operators associated with the conditional probability density given by (4):

$$\begin{aligned} \tilde{M}^{(k)} &= xP_k^0 \otimes P_k^0 + yP_k^1 \otimes P_k^1 + XP_k^1 \otimes P_k^0 + X'P_k^1 \otimes P_k^1 \\ &+ B_1 P_k^0 \otimes (T_k^{01} + T_k^{10}) + B_2 P_k^1 \otimes (T_k^{01} + T_k^{10}) \\ &+ B_3 (T_k^{01} + T_k^{10}) \otimes P_k^0 + B_4 (T_k^{01} + T_k^{10}) \otimes P_k^1 \\ &+ B_5 (T_k^{01} + T_k^{10}) \otimes (T_k^{01} + T_k^{10}) \end{aligned} \quad (7)$$

with P_k^0 and T_k^{01} denoting projection and transfer operators in the configuration space. Various constants in (7) are defined through the following relations:

$$\begin{aligned} X &= x - \alpha(x - y), \\ X' &= y + \alpha(x - y), \\ B_1 &= x\sqrt{(1 - \alpha)y(x + \alpha y)} + y\sqrt{(1 - \alpha)x(y + \alpha x)}, \\ B_2 &= y\sqrt{(1 - \alpha)y(x + \alpha y)} + x\sqrt{(1 - \alpha)x(y + \alpha x)}, \\ B_3 &= \alpha\sqrt{xy}, \end{aligned} \quad (8)$$

$$B_4 = -\alpha\sqrt{xy},$$

$$B_5 = \sqrt{xy} (\sqrt{(1 - \alpha)y(x + \alpha y)} - x\sqrt{(1 - \alpha)x(y + \alpha x)}).$$

The augmented-space operator associated with independent probability density is given by

$$\tilde{M}^{(k)} = \{xP_k^0 + yP_k^1 + \sqrt{xy} (T_k^{01} + T_k^{10})\}. \quad (9)$$

We make explicit use of these operators and the central theorem for correlated random variables to set up an effective Hamiltonian in augmented space. We then use the recursion technique to be discussed in the next section to calculate the configuration-averaged Green function.

III. TB-LMTO AND THE AUGMENTED-SPACE RECURSION TECHNIQUE

The tight-binding linearized-muffin-tin orbitals¹⁴ (TB-LMTO) method provides a reasonably good starting point for the electronic structure calculation of disordered alloys. It has been shown previously¹³ that TB-LMTO coupled with the augmented-space recursion technique provides a reasonable description of the electronic structure of disordered alloys.

The linearized-muffin-tin orbitals method introduced by Andersen¹⁴ gives a simple yet accurate first-principles description of the electronic structure of solids. As is well known, the LMTO basis set is minimal and complete for the muffin-tin or atomic-sphere approximation (ASA) potential used for its construction, over an energy range of about one Rydberg around the energy node about which linearization is carried out. We shall use the tight-binding version of this formalism. This is obtained by truncating a power-series expansion of a matrix $h = H - E_v$, where H is an effective, two-center TB Hamiltonian and E_v is an arbitrary energy chosen at the node around which linearization is carried out. If this power series is truncated after the first-order term, the orthogonal Hamiltonian is approximated by a two-center TB Hamiltonian and the recursion method yields a density of states whose features have energy positions correct to the first-order in their distance from E_v . If on the other hand, the truncation is performed after the second-order term, the Hamiltonian is less sparse (having non-negligible matrix elements between fourth-nearest neighbors), but still tractable within the recursion method. The resulting density of states (DOS) have features whose positions are correct to second order in their distance from E_v . It has been shown that the first-order Hamiltonian provides an accurate description¹⁴ certainly for relatively narrow d bands below the Fermi level. However, if we wish to describe the higher-energy range of s and p bands, for example, in a transition metal or even broad d bands, we have to go at least to the second term in the expansion series for both the Hamiltonian and the overlap matrix.

The TB-LMTO and its implications have been discussed in great detail earlier.¹⁴ We shall quote here the final result and refer the reader to the above-referenced review articles for further details.

For binary AB alloys, the LMTO Hamiltonian in its most localized representation is given by

$$H = \sum_{iL} C_{iL} a_{iL}^\dagger a_{iL} + \sum_{iL} \sum_{jL'} \Delta_{iL}^{1/2} S_{L,L'}^{ij} \Delta_{jL'}^{1/2} a_{iL}^\dagger a_{iL}. \quad (10)$$

The summation over j extends over first- and second-nearest neighbors of i . The potential parameters C_{iL} and

$\Delta_{iL}^{1/2}$ take values C_{LA} , $\Delta_{LA}^{1/2}$ or C_{LB} , $\Delta_{LB}^{1/2}$, respectively, depending upon whether site i is occupied by the A or B atom. For substitutional alloys with negligible size mismatch between the constituents structure matrix S_{LL}^{ij} is not random.

The above Hamiltonian can be written in terms of the site-occupation variable n_i as

$$H = \sum C_{LB} a_{iL}^\dagger a_{iL} + \sum \delta C_L n_i a_{iL}^\dagger a_{iL} + \sum \sum (\Delta_{LB}^{1/2} + \delta \Delta_L^{1/2} n_i) S_{L,L'}^{ij} (\Delta_{LB}^{1/2} + \delta \Delta_L^{1/2} n_j) a_{iL}^\dagger a_{iL}. \quad (11)$$

δC_L and $\delta \Delta_L^{1/2}$ are the fluctuations of the potential parameters about the uniform background of the B component. n_i takes value 0 or 1 depending upon whether site i is occupied by the A or B atom. Now the nonrandom Hamiltonian \tilde{H} in the extended augmented space is constructed by replacing the random site occupation variable n_i by its corresponding operator representation $\tilde{M}^{(i)}$ in configuration space. Since we consider the short-range order to be restricted to the first-neighbor shell, only the operators corresponding to sites belonging to the first-neighbor shell contains the signature of the conditional probability while the operators belonging to other sites will have no short-ranged correlations. The operator $\tilde{M}^{(i)}$ is taken from Eqs. (2) and (4).

Substituting these $\tilde{M}^{(i)}$'s for n_i 's in the random Hamiltonian, the constructed nonrandom Hamiltonian \tilde{H} in the augmented space is obtained as

$$\begin{aligned} \tilde{H} = & \sum_{k,L} C_L^B a_k^\dagger a_k + \sum_{L} \sum_{k \neq NN1} \delta C_L \{ x P_k^0 + y P_k^1 + \sqrt{xy} (T_k^{01} + T_k^{10}) \} \\ & + \sum_{L} \sum_{k \in NN1} \delta C_L \{ x P_1^0 \otimes P_k^0 + y P_1^0 \otimes P_k^1 + X P_1^1 \otimes P_k^0 + X' P_1^1 \otimes P_k^1 + B_1 P_1^0 \otimes (T_k^{01} + T_k^{10}) + B_2 P_1^1 \otimes (T_k^{01} + T_k^{10}) \\ & + B_3 (T_k^{01} + T_k^{10}) \otimes P_k^0 + B_4 (T_k^{01} + T_k^{10}) \otimes P_k^1 + B_5 (T_1^{01} + T_1^{10}) \otimes (T_k^{01} + T_k^{10}) \} \\ & + \sum_{L,L'} \sum_{k \neq NN1} \sum_{k' \neq NN1} [\Delta_{LB}^{1/2} + \delta \Delta_L^{1/2} \{ x P_k^0 + y P_k^1 + \sqrt{xy} (T_k^{01} + T_k^{10}) \}] \cdots \\ & \quad \times S_{LL'}^{kk'} [\Delta_{LB}^{1/2} + \delta \Delta_L^{1/2} \{ x P_k^0 + y P_k^1 + \sqrt{xy} (T_k^{01} + T_k^{10}) \}] \\ & + \sum_{L,L'} \sum_{k=1} \sum_{k' \in NN1} [\Delta_{LB}^{1/2} + \delta \Delta_L^{1/2} \{ x P_k^0 + y P_k^1 + \sqrt{xy} (T_k^{01} + T_k^{10}) \}] \\ & \quad \times S_{LL'}^{kk'} [\Delta_{LB}^{1/2} + \delta \Delta_L^{1/2} \{ x P_1^0 \otimes P_k^0 + y P_1^0 \otimes P_k^1 \\ & \quad + X P_1^1 \otimes P_k^0 + X' P_1^1 \otimes P_k^1 + B_1 P_1^0 \otimes (T_k^{01} + T_k^{10}) + B_2 P_1^1 \otimes (T_k^{01} + T_k^{10}) \\ & \quad + B_3 (T_k^{01} + T_k^{10}) \otimes P_k^0 + B_4 (T_k^{01} + T_k^{10}) \otimes P_k^1 + B_5 (T_1^{01} + T_1^{10}) \otimes (T_k^{01} + T_k^{10}) \}]. \end{aligned} \quad (12)$$

Once the effective Hamiltonian has been constructed, the generalized augmented-space theorem gives the configuration averaged Green function to be

$$\langle G \rangle_{av} = \langle v_0 | (E\tilde{I} - \tilde{H})^{-1} | v_0 \rangle.$$

The recursion method of Haydock *et al.*¹² provides an algorithm for calculating diagonal matrix element of the resolvent or Green function associated with the Hamiltonian \tilde{H} . Beginning with a starting state $|\xi_1\rangle = |R_i, l\rangle \otimes |\Psi_0\rangle$ where Ψ_0 is the string of zero's representing the *ground state* $|v_0\rangle$ of the full system configuration space Φ , one generates a discrete chain of mutually orthogonal vectors $|\xi_i\rangle$ through the three-term recursion,

$$\begin{aligned} H|\xi_n\rangle &= \alpha_n |\xi_n\rangle + \beta_{n+1} |\xi_{n+1}\rangle + \beta_n |\xi_{n-1}\rangle, \\ \alpha_n &= \langle \xi_n | \otimes \tilde{H} | \xi_n \rangle, \\ \beta_n &= \langle \xi_{n-1} | \otimes \tilde{H} | \xi_n \rangle, \end{aligned}$$

where the inner product in real space is defined as

$$\langle m | \otimes | n \rangle = C_m^\dagger C_n = \delta_{mn}.$$

The basis $|m\rangle$ is represented by a column vector C_m with zeros everywhere except at the m th position. The inner product between the basis vectors in configuration space is

$$B[C, \{S_C\}] \otimes B[C', \{S_{C'}\}] = \delta_{CC'} \delta_{\{S_C, S_{C'}\}},$$

where C is the number of 1's in configuration space, called the cardinality of the basis and sequence of positions where one has 1's $\{S_C\}$, called the cardinality sequence, labels the basis.

This prescription transforms the Hamiltonian into tri-diagonal form and thus leads directly to a continued fraction representation for the diagonal element of the averaged Green function. If the algorithm is stopped after N steps, N exact levels of the continued fraction are ob-

tained. A Herglotz terminator $T_L(E)$ is substituted for the remaining part of the continued fraction. This terminator reflects the asymptotic properties of the continued fraction accurately. Such a termination procedure retains the Herglotz properties of the Green function. It maintains the correct bandwidths, band weights, and the correct singularity at the band edges. In order to reduce the necessary amount of computer storage and make the computation faster, explicit use of point-group symmetry operation and bit manipulation technique of the spin- $\frac{1}{2}$ Ising model computational methodology has been used, a point that will be discussed in the next section.

IV. COMPUTATIONAL DETAILS

As discussed in an earlier section, the ASA form of the orthonormalized LMTO Hamiltonian with the expansion truncated after the first term [which is of first order in $(E - E_\nu)$, where the E_ν 's have been chosen at the center of the bands] is used to parametrize the constituent Hamiltonians. The density of states has been found by the recursion method with the augmented-space effective Hamiltonian representing the random distribution of sites described by either ASA-LMTO Hamiltonian of A constituent or B constituent. The augmented-space map is generated from a real-space cluster of 400 atoms. We have generated a sequence of eight pairs of continued fraction coefficients for s , p , and d states. The Herglotz terminator is now generated given the prescription of Haydock and Nex¹⁶ and Lucini and Nex.¹⁷ Details of this are given in the Appendix.

The screened structure matrix $S_{LL'}^{ij}$ is found by direct inversion of the cluster containing 19 nearby atoms. We have used the spd set of screening parameters ($Q_s^\alpha = 0.3485$, $Q_p^\alpha = 0.0503$, $Q_d^\alpha = 0.01071$, $Q_{>2}^\alpha = 0$) to get the most localized version of the TB-LMTO Hamiltonian.

A major objection against the implementation of calculations based on the augmented-space formalism was that there was no general and efficient method for storing only the immediately accessible vectors in the augmented hyperspace. These are, for example, 2^{13} in number for a system consisting of A or B atoms in a cluster of a central site and its 12 nearest neighbors (the simplest cluster for modeling a fcc binary alloy). We present the computational developments that have been made to make the implementation feasible. Since this has already been described elsewhere in detail¹³ we only briefly mention the salient points here.

The first step is the reduction of the Hamiltonian by exploiting the symmetries of the underlying lattice. The Hamiltonian described by (10) contains the information of both the structure of the underlying lattice and the symmetry of the orbitals. It has been shown by Gallagher¹⁸ that if the starting state of the recursion belongs to an irreducible representation of the Hamiltonian, then the states generated in the process of recursion belong to the same row of the same irreducible representation of the Hamiltonian. Further the recursions with the starting state corresponding to the different rows of the same irreducible representation are similar. The states belong-

ing to the different irreducible representations or different rows of the same irreducible representation do not mix. So we need to retain only those states for the purpose of recursion and get the same resolution as with all of them. The recursion is done only with those states which are not related to one another by the point-group symmetry of the underlying lattice. Once these state vectors are identified, the recursion can be performed in the reduced space, modified with weight factors. Thus, in the computation we need far less storage and time because the dimensionality of the matrix H is reduced drastically.

In practice a starting site is chosen. The number of distinct equivalent sites, related to the starting site by the local point-group symmetry, constitutes the weight of the starting site. As discussed earlier, in the process of recursion, these equivalent sites are not considered, and the calculation is confined only to the nonequivalent sites. For example, for an s -state Hamiltonian on a lattice with cubic symmetry, all the nonequivalent sites are confined to $\frac{1}{48}$ th of the entire lattice. Inclusion of p orbitals introduces preferred x , y , or z directions and breaks the symmetry between the x , y , and z axes. Thus, the point-group symmetry operations which interchange between x , y , and z coordinates are prohibited. Hence the irreducible part of the lattice instead of being $\frac{1}{48}$ th of the entire lattice now becomes one-eighth. If with each site R we attach weight W_R , which is given by the number of basis states equivalent to $|R\rangle$, then the whole process can be summarized as follows: In the new TB-LMTO reduced basis we have

$$\langle R, L | H | R, L \rangle = C_{R,L}, \quad (13)$$

$$\begin{aligned} \langle R', L' | H | R, L \rangle \\ = \sqrt{(W_R / W_{R'})} \Delta_{R'L}^{1/2} S_{R',L',R,L}^\alpha \Delta_{R,L}^{1/2} \beta_R(L, L'), \end{aligned} \quad (14)$$

where R and R' both belong to the irreducible part of the lattice. $\beta_R(L, L')$ is the factor which can be either 0 or 1, depending on whether the position occupied by the site R is a symmetry position with respect to orbitals L and L' or not. This fact can be made more transparent in the following way: The structure matrix element connecting two orbitals occupying the two different sites is given by the two-center Slater-Koster integrals. Apart from a factor made of π and σ integrals the Slater-Koster integral contains a factor made up of direction cosines of the vector joining the two basis states between which the matrix element is taken. It reflects the symmetry property of the overlapping orbitals. Now for the different equivalent sites connected to a given site, this direction cosine has different signs. In the effective irreducible basis, which is a linear combination of the old basis, a particular linear combination may give rise to a zero Hamiltonian matrix element. We shall call these positions, where such zero matrix elements occur, *the symmetry positions* with respect to orbitals L and L' . The representation of the Hamiltonian in terms of the irreducible basis sets reduces the rank of the Hamiltonian matrix. The workload of the recursion reduces drastically.

In spite of the reduction in real space, the dimension of

the full augmented space is still very large: $N \times 2^N$ for a system reduced to nonequivalent N sites and disorder characterized by a binary probability distribution. However, in analogy to real-space symmetry, if we exploit the symmetry of the configuration space which arises due to homogeneity of disorder, then the rank of the augmented space is reduced further and the augmented-space recursion becomes tractable. This basic step of identifying a set of nonequivalent vectors and their weights can be achieved in the following way: Since the augmented space is a direct product of the real space and the configuration space, which are disjoint, symmetry operations on either of them apply independently of each other. For example, if a site is occupied by an A atom, then all the Z configurations in which its $(Z-1)$ neighbors are occupied by A atoms and one by B are equivalent. In practice, a site in the augmented space is chosen as $|R, \{C, \{S_C\}\}\rangle$. All the equivalent sites are obtained by point-group operation \mathcal{R} on the site in question:

$$\begin{aligned} |R', \{C', \{S_{C'}\}\}\rangle &= \mathcal{R} |R, \{C, \{S_C\}\}\rangle \\ &= \mathcal{R} R, \mathcal{R}[C, \{S_C\}\rangle . \end{aligned}$$

The number of distinct sites obtained in this way is the weight of the site in question. As in the real-space recursion only the nonequivalent (NE) sites obtained in this way are retained for the purpose of recursion. Once we have defined the Hamiltonian, and its operation in augmented space, the recursion method on the augmented space gives the configuration-averaged Green function directly.

Another important step is the reduction of computer storage and making the computation faster by identification of various operations in configuration space of a binary alloy with Ising computational technology and use of logical operations to describe the action of augmented-space Hamiltonian. As we have already indicated, each basis in configuration space is nothing but a string of 0's and 1's, where the sequence of positions where we have 1's is the *cardinality sequence*. We may thus represent the basis vectors by a collection of binary words. In an M -bit machine, each M -bit word can represent up to $M-1$ terms as a sequence of 0's and 1's and for the configuration of a lattice size N , $N/(M-1)$ words are necessary. All operations of the augmented-space Hamiltonian on the states in the augmented space reduce to bit manipulation and logical operations on the M -bit words representing the basis vectors.¹⁹

V. RESULTS AND DISCUSSION

In this section we present the electronic structure calculation of the AgPd alloy and paramagnetic FeNi alloy with local order present in them. The effect of short-range order on both the AgPd alloy and paramagnetic FeNi alloy has been studied earlier with two different methodologies KKR-CPA-ECM (Ref. 20) and the surrounded atom model,²¹ respectively. We have intentionally chosen these two systems in order to compare our result qualitatively with that obtained by two other methodologies. Furthermore AgPd is the simplest alloy to start

with a negligible charge transfer effect and small mismatch between the constituent's Wigner-Seitz radii. The same is true for the FeNi system. So approximate treatment of charge self-consistency can be made by utilizing the flexibility in the choice of sizes of the atomic spheres, a point extensively discussed by Kudronovský and Drachal.²²

We first present our calculations for a cluster of impurity atoms embedded in a translationally invariant medium. These density of states can be directly compared with that obtained by the embedded-cluster method. The translationally invariant medium outside the embedded cluster in the case of KKR-CPA-ECM is a single-site-averaged CPA while the translationally invariant medium used in the present study is obtained by the augmented-space recursion technique. Figure 1 shows density of states in a 50-50 AgPd alloy associated with a Ag atom surrounded by [Fig. 1(a)] Pd and [Fig. 1(b)] Ag atoms and a Pd atom surrounded by [Fig. 1(c)] Ag and [Fig. 1(d)] Pd atoms in the first-neighbor shell. We find that similar to the KKR-CPA-ECM study that local environment fluctuation has a significant influence on the site-decomposed density of states. The density of states of Ag and Pd clusters [Figs. 1(b) and 1(d)] resemble those

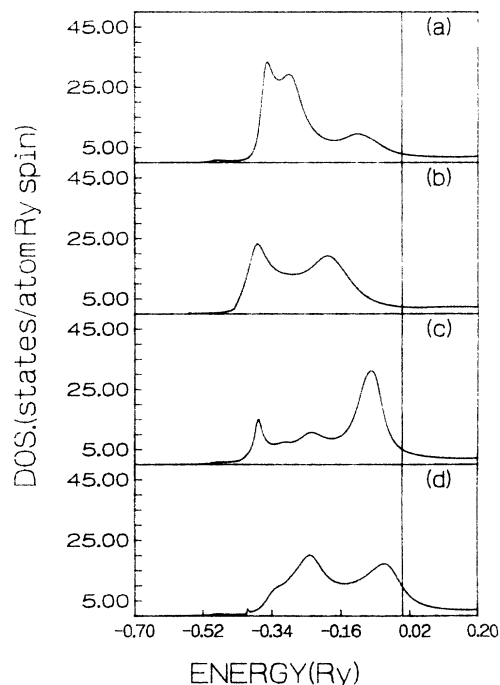


FIG. 1. The densities of states of a $\text{Ag}_{50}\text{Pd}_{50}$ alloy: (a) on a Ag site, surrounded by Pd atoms in a nearest-neighbor shell, (b) on a Ag site surrounded by Ag atoms in its nearest-neighbor shell, (c) on a Pd atom surrounded by Ag atoms in its nearest-neighbor shell, (d) on a Pd atom surrounded by Pd atoms in its nearest-neighbor shell. The energies are measured from the Fermi level.

of pure Pd and Ag with characteristic two-peaked structure. Whereas single peaks characterizing the virtual-level impurity peak are obtained in the density of states of a Ag atom surrounded by 12 Pd atoms and a Pd atom surrounded by 12 Ag atoms as in Figs. 1(a) and 1(c).

In Fig. 2, we present the configuration-averaged density of states for different values of the short-range order parameter α varying between 1.0 and -1.0 . This is the full range of variation possible for α at 50-50 concentration. The results show a regular variation of density of states as a function of a short-range order parameter which is the deciding factor for the local environment. Furthermore for $\alpha=1$ and -1 , we obtain the asymptotic limit where only one configuration of the embedded cluster is possible. For $\alpha=1$ the configuration is given by a cluster containing all like atoms while for $\alpha=-1$, the configuration is given by a cluster in which the central atom is surrounded by all unlike atoms. In other words, one gives complete segregation and the other gives complete ordering. Putting these values of α in Eq. (12), it is easy to check that the Hamiltonian reduces to the embedding cluster Hamiltonian. The generalized augmented-space formalism is therefore exact in these limits. It is interesting to note that we do not get any violation of Herglowitzicity in the whole range of α . This is in contrast to negative density of states found for the model case by Razez and Prasad, particularly in the extreme value ranges of α .

Figures 3 and 4 are exactly the analogous studies for the paramagnetic 50-50 FeNi alloy. Figure 3 gives the embedding-cluster density of states for Ni and Fe atoms

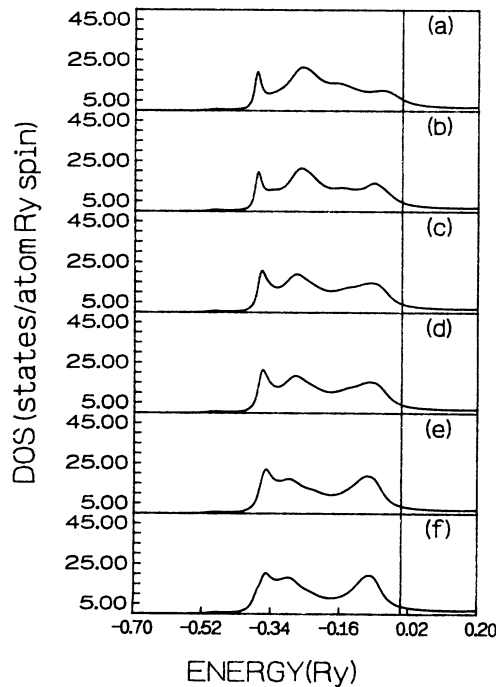


FIG. 2. The density of states of a $Ag_{50}Pd_{50}$ alloy with Warren-Cowley parameter α : (a) 1.0, (b) 0.5, (c) 0.1, (d) -0.1 , (e) -0.5 , (f) -1.0 . The energies are measured from the Fermi level.

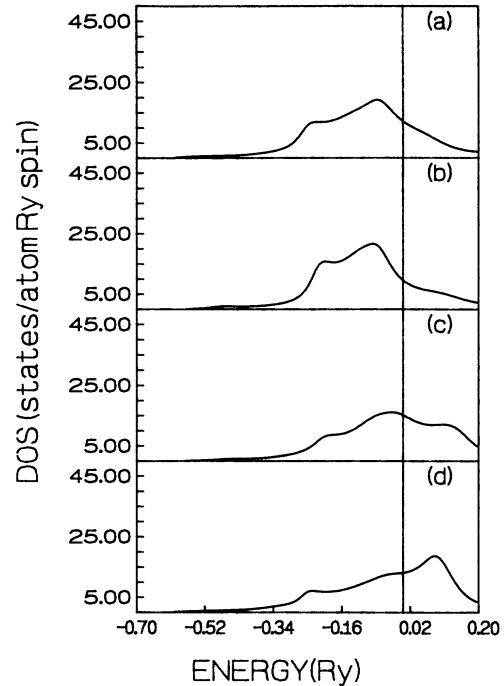


FIG. 3. The density of states of a paramagnetic $Fe_{50}Ni_{50}$ alloy: (a) on a Ni site surrounded by Ni atoms in its nearest-neighbor shell, (b) on a Ni site surrounded by Fe atoms in its nearest-neighbor shell, (c) on a Fe site surrounded by Ni atoms in its nearest-neighbor shell, (d) on a Fe site surrounded by Fe atoms in its nearest-neighbor shell. The energies are measured from the Fermi level.

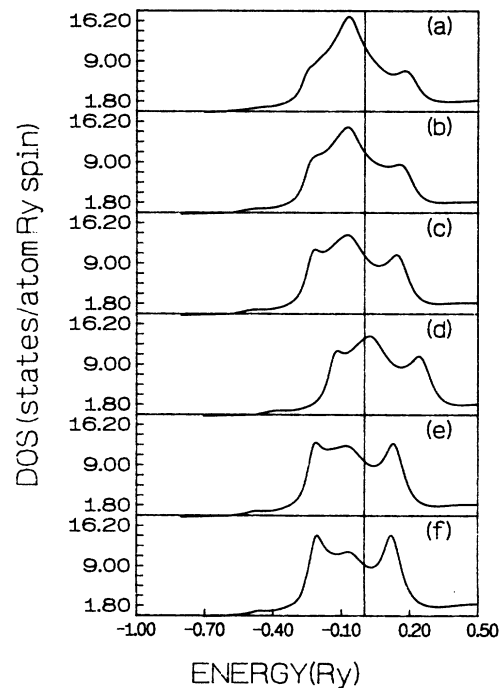


FIG. 4. The density of states of an $Fe_{50}Ni_{50}$ alloy with Warren-Cowley parameter α : (a) 1.0, (b) 0.5, (c) 0.1, (d) -0.1 , (e) -0.5 , (f) -1.0 . The energies are measured from the Fermi level.

surrounded by similar or different species, while Fig. 4 gives the variation of the density of states as α varies from 1.0 to -1.0 . Our conclusions are the same as for the 50-50 AgPd alloy.

For AgPd alloys, since there is only a negligible amount of charge transfer, it is reasonable to assume in a first approximation that the total energy of the system is dominated by the band-structure energy and to neglect the intrasphere interaction energy term. In Fig. 5(a) we present the variation of band-structure energy with a short-range order parameter. The curve clearly shows a tendency towards ordering. The same ordering tendency has been predicted by the KKR-CPA-ECM (Ref. 20) study. However, the ordering tendency is not experimentally observed in 50-50 AgPd. It has been argued that the formation of the ordered structure in AgPd is prevented by slow diffusion rates. The confirmation of this assumption is beyond the scope of this work.

The variation of the band-structure energy with a short-range order parameter for paramagnetic 50-50 FeNi is shown in Fig. 5(b) and it clearly shows a tendency towards phase segregation. This prediction agrees with that obtained by the surrounded atom model²¹ incorporating severe simplification like substitution of a Bethe lattice for the proper crystal structure of the material surrounding the cluster. The surrounded atom treatment leads to segregation for Fe₅₀Ni₅₀. On the contrary for Ni-rich FeNi alloys, the Cowly order parameter became negative and tendency to ordering was predicted.

In summary these initial results for AgPd and paramagnetic FeNi shows a tendency towards order in

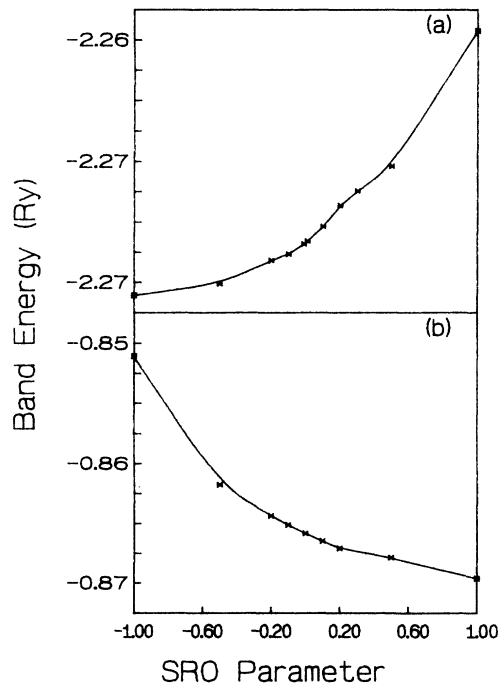


FIG. 5. The variation of band energy as a function of the Warren-Cowley parameter for (a) Ag₅₀Pd₅₀ and (b) paramagnetic Fe₅₀Ni₅₀. The energies are measured from the Fermi level.

the former and a tendency towards segregation in the latter case which are in agreement with previous theoretical studies using other methodologies. The generalized augmented-space formalism coupled with the recursion technique provides a reliable and computationally implementable methodology for treating alloys with local fluctuation effects present. Investigations with other alloy systems are now under preparation. Attempts are also presently made to carry the full charge self-consistency within the local-density approximation, so that the total energies rather than band energies can be obtained for various values of short-range order parameter. Once such a self-consistency is obtained we can then compare the short-range order parameter predicted by our theory with that obtained by x-ray and neutron-diffraction data.

APPENDIX: THE TERMINATOR

The generation of the terminator has been described in detail by Haydock and Nex.¹⁶ We shall give the general outline here.

A set of coefficients $\{\alpha_n, \beta_n\}$ is first generated recursively from

$$\beta_{n+1}|\psi_{n+1}\rangle = \tilde{H}|\psi_n\rangle - \alpha_n|\psi_n\rangle - \beta_n|\psi_{n-1}\rangle,$$

where

$$\alpha_n = \langle \psi_n | \odot \tilde{H} | \psi_n \rangle,$$

$$\beta_n = \langle \psi_{n-1} | \odot \tilde{H} | \psi_n \rangle.$$

We generate up to $n = n_1$ steps. We now generate orthogonal polynomials of the first and second kinds: $P_n(z)$ and $Q_n(z)$ for the above recurrence relation. These are solutions of

$$P_{n+1}(z) = (z - \alpha_n)P_n(z) - \beta_n^2 P_{n-1}(z),$$

$$Q_n(z) = (z - \alpha_n)Q_{n-1}(z) - \beta_n^2 Q_{n-2}(z),$$

with $P_{-1} = 0 = Q_{-1}$, $P_0 = 1 = Q_0$.

The next step is to accurately locate, from the generated continued fraction coefficients $n < n_1$, the lower band edge a , the bandwidth r , and the band weight w . From this we construct a model Herglotz function:

$$F(z) = 8w[z - (a + r/2) - \sqrt{(z - a)(z - a - r)}]/r^2.$$

The *terminator coefficients*, which are the coefficients of the continued fraction expansion of $F(z)$, are $\alpha_t = a + r/2$ and $\beta_t = r/4$. Lucini and Nex¹⁷ now interpolate between the computed coefficients and those of the analytic terminator in the following manner:

$$\alpha_n = \begin{cases} \alpha_n, & n \leq n_1, \\ [\alpha_n(n_2 - n) + \alpha_t(n - n_1)/(n_2 - n_1)], & n_1 < n \leq n_2, \\ \alpha_t, & n > n_2. \end{cases}$$

The method is analogous to splicing as opposed to butt-joining pieces of wood.

We now run the recursion again with \tilde{H} replaced by z , the state vectors by polynomials, and the inner product by a union of Gauss-Chebyshev quadrature:

$$f(z) \odot g(z) = \sum_{i=1}^n \omega_i f(\alpha'_i) g(\alpha'_i),$$

where

$$\omega_i = \frac{\pi w}{n+1} \sin^2 \vartheta_i,$$

$$\alpha'_i = \alpha_i + (1 - \cos \vartheta_i) r / 2,$$

$$\vartheta_i = \pi \frac{i}{n+1}.$$

This will generate a set of recursion coefficients $\{\gamma_n, \delta_n\}$ and a set of mutually orthogonal polynomials $\{R_n(z)\}$ and $\{S_n(z)\}$. The terminator is given by

$$T(z) = \frac{S_{n_2-2}(z) - F(z)R_{n_2-1}(z)}{\delta_{n_2-1}^2 [S_{n_2-3}(z) - F(z)R_{n_2-2}(z)]}.$$

Again from the fact that R_n and S_n are polynomials of order n and $F(z)$ is a Herglotz function, it follows immediately that the terminator is itself Herglotz.²³

The Green function is given by

$$G(z) = \frac{Q_{n_2-2}(z) - \beta_{n_2-1}^{12} T(z) Q_{n_2-3}}{P_{n_2-1}(z) - \beta_{n_2}^2 T(z) P_{n_2-2}}.$$

Using very similar arguments as before, the Green function is Herglotz if $T(z)$ is Herglotz.

It has been shown earlier²³ that moments of the Green function of order m can be expressed in terms of α_n and β_n for $n \leq m$. Since the coefficients up to $n = n_2$ are exact, it follows that all moments up to order n_2 are exact in this approximation.

¹P. Soven, Phys. Rev. **156**, 809 (1967).

²M. Tsukada, J. Phys. Soc. Jpn. **32**, 1475 (1972).

³F. Cyrot-Lackmann and M. Cyrot, Solid State Commun. **22**, 517 (1977).

⁴A. Gonis and J. W. Garland, Phys. Rev. B **16**, 2424 (1977).

⁵A. Mookerjee, J. Phys. C **6**, 1340 (1973).

⁶A complex function $f(z)$ is said to be Herglotz if (i) the singularities of $f(z)$ lie on the real z axis; (ii) $\text{Im}f(z) \leq 0$ for $\text{Im}z > 0$, $\text{Im}f(z) \geq 0$, for $\text{Im}z < 0$; and (iii) $f(z) \sim 1/z$ as $z \rightarrow \infty$ on the real axis.

⁷A. Mookerjee, J. Phys. F **17**, 1511 (1987); S. S. Rajput, S. S. A. Razee, A. Mookerjee, and R. Prasad, J. Phys.: Condens. Matter **2**, 2653 (1990); S. S. A. Razee, S. S. Rajput, A. Mookerjee, and R. Prasad, Phys. Rev. B **42**, 9391 (1990).

⁸A. Datta, P. K. Thakur, and A. Mookerjee, Phys. Rev. B **48**, 8567 (1993).

⁹L. J. Gray and T. Kaplan, Phys. Rev. B **14**, 3462 (1976); **15**, 3260 (1977).

¹⁰S. S. A. Razee and R. Prasad, Phys. Rev. B **48**, 1349 (1993).

¹¹A. Mookerjee and R. Prasad, Phys. Rev. B **48**, 17724 (1993).

¹²R. Haydock, V. Heine, and M. J. Kelly, J. Phys. C **5**, 2845

(1972).

¹³T. Saha, I. Dasgupta, and A. Mookerjee, J. Phys.: Condens. Matter **6**, L245 (1994).

¹⁴O. K. Andersen and O. Jepsen, Phys. Rev. Lett. **53**, 2571 (1984); G. P. Das, Pramana **38**, 545 (1992).

¹⁵H. J. Nowak, O. K. Andersen, T. Fujiwara, O. Jepsen, and P. Vargas, Phys. Rev. B **44**, 3577 (1991).

¹⁶R. Haydock and C. M. M. Nex, J. Phys. C **17**, 4788 (1984).

¹⁷M. U. Lucini and C. M. M. Nex, J. Phys. C **20**, 3125 (1987).

¹⁸J. Gallagher, Ph.D. thesis, University of Cambridge, U.K., 1978.

¹⁹A. Datta and A. Mookerjee, Int. J. Mod. Phys. B **6**, 3295 (1992).

²⁰A. Gonis, W. H. Butler, and G. M. Stocks, Phys. Rev. Lett. **50**, 1482 (1983).

²¹M. Cyrot, F. Cyrot-Lackmann, M. C. Desjonquères, and J. P. Gaspard, J. Phys. (Paris) Colloq. **38**, C7-285 (1977).

²²J. Kudrnovský and V. Drchal, Phys. Rev. B **41**, 7515 (1990).

²³J. A. Shohat and J. D. Tamarkin, *Problem of Moments* (American Mathematical Society, Providence, Rhode Island, 1950).